INTERNATIONAL JOURNAL FOR NUMERICAL METHODS IN FLUIDS, VOL. 11, 209–226 (1990)

SIMPLE TEST CALCULATIONS CONCERNING FINITE ELEMENT APPLICATIONS TO NUMERICAL WEATHER PREDICTION

J. STEPPELER*

ECMWF, Shinfield Park, Reading, U.K.

SUMMARY

Different finite element schemes are investigated with respect to their application in numerical weather prediction. Different methods of staggering of variables are considered. The tests concern the accuracy of a Rossby wave prediction and the generation of noise in a geostrophic adjustment process. Theoretical results concerning the noise level of different schemes are confirmed by computations with a one-dimensional model. Favourable results were obtained by hybrid schemes, using different Galerkin treatments for different terms of the dynamic equations.

KEY WORDS Finite elements Atmospheric flow Petrov–Galerkin Staggered grids Hybrid scheme

1. INTRODUCTION

In numerical models of the atmosphere an accurate treatment of transient features of the flow is essential. This leads to the requirement of a reasonable order of the discretization. The finite element method is able to obtain a high degree of accuracy, as shown in Reference 1. Atmospheric models based on this method are described in References 2–4.

Another important aspect of atmospheric models is the occurrence of a stationary or very slowly varying part of the flow. This represents the climate of the model and is caused by a balance of forcing and different transport processes. Associated with this is the problem of geostrophic adjustment.

In this respect the numerical properties of an atmospheric model may be analysed by similar considerations as aeronautical applications of finite elements, where the stationary flow is of interest. For such applications a number of finite element applications suffer from noise problems. This leads to the requirement of mixed interpolation,[5,6] meaning different choices of finite element representations for the pressure and velocity variables.

As pointed out in References 7 and 8, the requirement for mixed interpolation for finite element schemes in stationary flow applications is associated with the requirement for staggered grids in meteorological models.[9,10] This latter requirement is the result both of practical experience in numerical weather prediction and of theoretical analysis based on the transfer function analysis of

* Present address: National Meteorological Center 2, World Weather Building, Camp Springs–Maryland, Washington, DC 20233, U.S.A.

0271–2091/90/100209–18$09.00

Received 17 March 1989
Revised 19 October 1989

gravity waves.[9] The request for staggered grids is valid both for finite element and finite difference discretizations.[9,10]

In the context of finite element discretizations a staggering of the grid can be achieved in different ways. We consider here the possibility of using a combination of linear and piecewise constant elements.[7,8] A drawback of these methods is a possible degradation of accuracy, since part of the discretization uses low-order basis functions. This will be investigated by predictions of a one-dimensional Rossby wave.

It is intriguing to combine the positive effects of different methods by combining different ways of staggering. In this way hybrid schemes are obtained which are based on the simultaneous application of two different grids. Theoretical results[10] indicate that the staggered grid will be necessary for the treatment of the gravity terms. Accuracy considerations[1] suggest an unstaggered treatment for the advection terms. Simple hybrid schemes are obtained by using Petrov–Galerkin methods for gravity wave terms. An example of this kind is given in Reference 11. In the present paper we investigate schemes which use a combination of an Arakawa[12] C- and A-grid. Hybrid schemes based on Petrov–Galerkin and back-transformation methods will be investigated.

The example of a one-dimensional flow with mountain forcing will be used to investigate the geostrophic adjustment process. The results essentially confirm theoretical expectations.

All applications of finite elements or finite differences to numerical weather prediction use regular grids or grids with a smoothly varying grid length,[13] with the notable exception of the model by Phillips[14] which refines the grid by a factor of two. Much of the work with finite element models for numerical weather prediction is comparatively old and uses uniform interpolation on an Arakawa A-grid.

In the present paper the suitability of different schemes for variable resolution is investigated. We consider the situation that the grid length is suddenly reduced by a factor of two. One-dimensional experiments seem suitable to establish necessary conditions on the applicability of such a scheme.

In the present paper the element functions have an order not higher than unity. The investigation of higher-order elements for horizontal discretization of atmospheric models is left for future investigations. For the vertical discretization, finite element schemes with linear,[15,25] quadratic[16] and cubic spline[17] basis functions have been used in numerical weather prediction. In particular, schemes using quadratic basis functions are worth investigating, since the numerical cost of the schemes[15,16] was approximately the same and, according to Reference 1, quadratic elements have a much better accuracy.

2. BASIC EQUATIONS

In order to test the horizontal discretization for atmospheric models we use the shallow water equations

$$\begin{aligned} \frac{\partial}{\partial t} U &= -UU_X - VU_Y - H_X + fV, \\ \frac{\partial}{\partial t} V &= -UV_X - VV_Y - H_Y - fU, \\ \frac{\partial}{\partial t} H &= -((H - F_0)U)_X - ((H - F_0)V)_Y, \end{aligned} \tag{1}$$

where U and V are the velocity components in the X- and Y-direction respectively, H is the height of the free surface, F_0 is the orographic forcing field and f is the Coriolis parameter.

An alternative form of (1) uses vorticity and divergence as independent model variables. These equations have been used successfully for atmospheric modelling.[13] A transfer function analysis[10] shows that this form of the shallow water equations can be used with unstaggered meshes. There is, however, some incentive to use the primitive equations (1), since the discretization will be simpler and use less computation time. In particular, the introduction of semi-Lagrangian methods makes it desirable to use the primitive equations.[11]

A one-dimensional form of (1) is obtained as

$$\begin{aligned} \frac{\partial}{\partial t} U &= -UU_X + fV - H_X, \\ \frac{\partial}{\partial t} V &= -UV_X - fU - H_Y^\circ, \\ \frac{\partial}{\partial t} H &= -((H - F_0)U)_X, \end{aligned} \tag{2}$$

with H_Y° being a constant. An exact solution of (2) is the Rossby wave, which for an arbitrary choice of the function H_0 is defined as

$$\begin{aligned} H(X,t) &= H_0(X - U_0 t), \\ U(X,t) &= -H_Y^\circ/f = U_0 = \text{constant}, \\ V(X,t) &= H_X/f, \\ F_0(X) &= 0. \end{aligned} \tag{3}$$

The reproduction of this solution will be used as an accuracy test.

Wave solutions of (3) can be obtained by using $H(X,t) = \exp[\mathrm{i}(kX - \nu t)]$, with ν being the Rossby wave frequency and k the wave number. From (3) we derive $\nu = U_0 k$. For the phase velocity $C_p = \nu/k$ and the group velocity $C_g = \partial\nu/\partial k$ we obtain $C_p = C_g = U_0$. This means that there is no wave dispersion.

Another test problem will be the stationary equations obtained from (2) in the presence of a mountain:

$$\begin{aligned} 0 &= -UU_X + fV - H_X, \\ 0 &= -UV_X - fU - H_Y^\circ, \\ 0 &= ((H - F_0)U)_X. \end{aligned} \tag{4}$$

For our test problem we will choose a mountain forcing function F_0 which will be different from zero at just one grid point. Let us introduce for (2) the short notation

$$\frac{\partial}{\partial t}\psi(X) = \mathrm{RS}(\psi(X), \psi_X(X), \ldots), \tag{5}$$

where (5) represents one of the equations of motion in (2).

The finite element approximation tries to find approximate solutions for (5) of the form

$$\tilde{\psi}(X) = \sum_\rho \psi_\rho C_\rho(X), \tag{6}$$

where the ψ_ρ are the amplitudes of the representation, which determine an approximated model state for a given time, and the $C_\rho(X)$ are the basis functions of the scheme. The index ρ counts the different degrees of freedom or amplitudes of the scheme.

The standard Galerkin approximation of (5) provides prognostic equations for the ψ_ρ:

$$\sum_\rho \dot{\psi}_\rho(C_\rho, C_\beta) = (\mathrm{RS}, C_\beta), \tag{7}$$

with

$$(a, b) = \int \mathrm{d}X a(X) b(X).$$

Equation (7) is an implicit equation for the amplitude tendencies $\dot{\psi}_\rho$, which can be solved efficiently by Gaussian elimination.

An alternative to (7) is the Petrov–Galerkin method:

$$\sum_\rho \dot{\psi}_\rho(C_\rho, \bar{C}_\beta) = (\mathrm{RS}, \bar{C}_\beta). \tag{8}$$

Where the $\bar{C}_\beta$ represent any set of linear independent functions, not necessarily identical to the basis functions C_β.

We consider two choices, χ_ν and e_ν, for the basis functions C_ν, or $\bar{C}_\nu$, which are shown in Figure 1. The e_ν lead to piecewise linear interpolation and the χ_ν lead to piecewise constant interpolation in one space dimension. With the basis e_ν we will use integer values for the index ν, and with χ_ν the ν will be half-integer values $\nu = \rho + \frac{1}{2}$ with ρ having integer values. For such basis functions the amplitudes are also node point values defined at X_ν. The intervals $(X_\rho, X_{\rho+1})$ in Figure 1 are the elements. We will here always use the same one-dimensional elements $(X_\rho, X_{\rho+1})$ for the representation of the different fields, discarding the possibility of staggered elements, which were discussed in Reference 10. However, since with the basis functions χ_ν the natural definition of the amplitudes is on half-values $\nu = \rho + \frac{1}{2}$, a staggering is possible for the amplitudes, even though the elements are always unstaggered. The staggered schemes in two space dimensions were investigated in Reference 8.

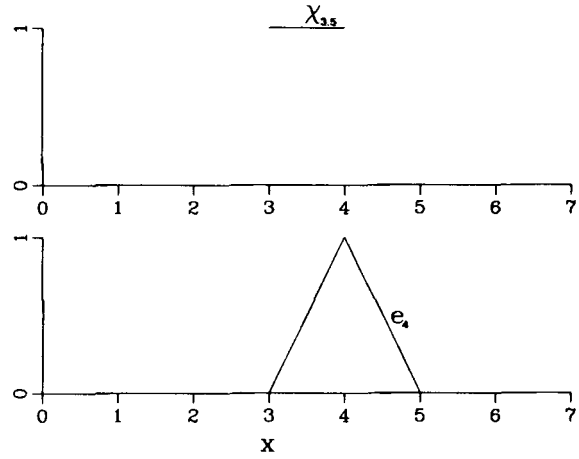

Figure 1. The basis functions e_ρ and $\chi_{\rho+1}$

3. DEFINITION OF NUMERICAL SCHEMES

The right-hand side of (2) may be split into two parts, the advection terms A and the gravity wave terms G:

$$\frac{\partial}{\partial t} U = U^A + U^G,$$

$$\frac{\partial}{\partial t} V = V^A + V^G, \tag{9}$$

$$\frac{\partial}{\partial t} H = H^A + H^G,$$

$$\begin{aligned} U^A &= -UU_X, & U^G &= -H_X + fV, \\ V^A &= -UV_X, & V^G &= -H_Y^o - fU, \\ H^A &= -UH_X, & H^G &= -UF_{oX} - (H - F_o)U_X. \end{aligned} \tag{10}$$

The physical significance of the two terms A and G is quite different, with the latter being responsible for gravity wave motion.

We will here investigate schemes 1–3 of the two-dimensional schemes defined in Reference 8. These are standard Galerkin schemes (7) which are defined if the basis function representation (6) is given. The basis function representations of schemes 1–3 are given in Table I. Only the piecewise linear basis functions $e_\nu(X)$ and the piecewise constant basis functions $\chi_{\rho+1/2}$ will be used. These schemes will be referred to as standard schemes 1, 2 or 3.

We will also investigate hybrid numerical schemes, which are obtained by applying different numerical approximations to terms A and G in (9) and (10). For such schemes we have instead of (7)

$$\dot{\psi}_\rho = \dot{\psi}_\rho^A + \dot{\psi}_\rho^G. \tag{11}$$

For the advection term $\dot{\psi}_\rho^A$ in the hybrid schemes we will always use standard Galerkin schemes with piecewise linear basis functions for all fields U, V, H. The standard representation of U, V, H will be by (6) with $C_\nu(X) = e_\nu(X)$:

$$\sum_\rho \dot{\psi}_\rho^A(e_\rho, e_\beta) = (\psi^A, e_\beta). \tag{12}$$

The choice of linear basis functions for the advection part of the tendency seems necessary because the motivation of hybrid schemes is to preserve the accuracy of the treatment of the advection term, which was demonstrated in Reference 1.

Table I. Basis function representation in one space dimension

	Basis function for		
Scheme	U	V	H
1	e_ρ	e_ρ	e_ρ
2	$\chi_{\rho+1/2}$	$\chi_{\rho+1/2}$	$\chi_{\rho+1/2}$
3	e_ρ	$\chi_{\rho+1/2}$	$\chi_{\rho+1/2}$

A theoretical analysis of advection discretization has been given in Reference 7. This is directly applicable to the discretization described above. Since here we use fourth-order discretization for all fields, we do not expect a dependence of the accuracy on the Rossby radius of deformation, as opposed to schemes discussed in Reference 7, which use highly accurate schemes only for some of the fields U, V, H. A rather extensive analysis of the advection terms has been given in Reference 18.

The simplest way to obtain a hybrid scheme is to define $\dot{\psi}_\rho^G$ by a Petrov–Galerkin method:

$$\sum_\rho \dot{\psi}_\rho^G (C_\rho, \bar{C}_\beta) = (\psi^G, \bar{C}_\beta), \tag{13}$$

with G being computed according to (10) using the piecewise linear representation (6) with $C_\rho(X) = e_\rho(X)$ for U, V, H. $\bar{C}_\beta$ in (13) may be any of the bases in Table I. The discretized equations are given by equations (13), (12), (11) and (10). With the basis belonging to scheme 1 the resulting Petrov–Galerkin scheme will be identical to scheme 1. The other two schemes we denote as schemes 2P and 3P. Scheme 2P is used in Reference 11. Since it results in an acceleration of gravity wave speeds, it requires a semi-implicit time discretization in order to be solved efficiently.

A necessary condition for the suitability of the numerical scheme is provided by the transfer function analysis.[9,10,19,20] A short introduction to this method is given in Appendix I. It analyses gravity waves as predicted by the numerical treatment of a linearized version of (1). A necessary condition to be required of a numerical scheme is that the group velocities of gravity waves in the numerical approximation have no sign reversal. For the standard Galerkin schemes 1, 2 and 3 such an analysis was given in Reference 8. Schemes 1 and 2 are unsuitable, which is in accordance with References 9 and 10, since these are unstaggered schemes. Scheme 3, however, gives positive group velocities for all directions of wave propagation. The Petrov–Galerkin scheme (13) is analysed in Appendix I and positive group velocities are obtained for schemes 2P and 3P, that is also for the unstaggered scheme 2P. In Section 4 test integrations using scheme 3P will be presented.

We will also use a transformation hybrid scheme which we will denote as scheme 3T. Again with this scheme the treatment of the advection term will be given by (12), and the representation of all fields is by the $e_\nu(X)$ basis according to (6). For the computation of the term G in (9) we will use a representation of U, V, H called $\bar{U}, \bar{V}, \bar{H}$ in the basic functions for scheme 3 in Table I:

$$\begin{aligned} \bar{U}(X) &= \sum_\rho \bar{U}_\rho e_\rho, \\ \bar{V}(X) &= \sum_\rho \bar{V}_{\rho+1/2} \chi_{\rho+1/2}, \\ \bar{H}(X) &= \sum_\rho \bar{H}_{\rho+1/2} \chi_{\rho+1/2}. \end{aligned} \tag{14}$$

The amplitudes $\bar{U}_\rho, \bar{V}_{\rho+1/2}, \bar{H}_{\rho+1/2}$ in (14) are obtained from the amplitudes U_ρ, V_ρ, H_ρ in the e_ρ representation by interpolation:

$$\bar{U}_\rho = U_\rho, \tag{15}$$

$$\bar{V}_{\rho+1/2} = \tfrac{1}{2}(V_\rho + V_{\rho+1}), \tag{16}$$

$$\bar{H}_{\rho+1/2} = \tfrac{1}{2}(H_\rho + H_{\rho+1/2}). \tag{17}$$

The averaging operation in (16) and (17) is invertible if the number of independent points V_ρ is uneven with periodic boundary condition. We denote this inverse operation by L^{-1}:

$$\begin{aligned} \{V_\rho\} &= L^{-1}\{\bar{V}_\rho\}, \\ \{H_\rho\} &= L^{-1}\{\bar{H}_\rho\}. \end{aligned} \tag{18}$$

Denote by $\bar{G}$ the term G in (10) computed by the representation (14). Then we compute the gravity wave term $\bar{G}^U_\rho$, $\bar{G}^V_{\rho+1/2}$, $\bar{G}^H_{\rho+1/2}$ in the representation (14) as

$$\begin{aligned} \sum_\rho \bar{U}^G_\rho(e_\rho, e_\beta) &= (\bar{U}^G e_\beta), \\ \sum_\rho \bar{V}^G_{\rho+1/2}(\chi_{\rho+1/2}, \chi_{\beta+1/2}) &= (V^G, \chi_{\beta+1/2}), \\ \sum_\rho \bar{H}^G_{\rho+1/2}(\chi_{\rho+1/2}, \chi_{\beta+1/2}) &= (\bar{G}^H, \chi_{\beta+1/2}). \end{aligned} \tag{19}$$

The $\dot{\psi}^G_\rho$ in (11) are then obtained by

$$\begin{aligned} U^G_\rho &= \bar{U}^G_\rho, \\ \{V^G_\rho\} &= L^{-1}\{\bar{V}^G_{\rho+1/2}\}, \\ \{H^G_\rho\} &= L^{-1}\{\bar{H}^G_{\rho+1/2}\}. \end{aligned} \tag{20}$$

4. NUMERICAL RESULTS

We use the one dimensional test problem defined in Equation (2). For spatial discretization we will use one of the schemes 1, 2, 3, 3P or 3T from Section 3. Schemes 1 and 2 are schemes with equal interpolation, or unstaggered schemes. Scheme 2 results from piecewise constant elements and is a second-order finite difference scheme. Scheme 1 uses linear elements and provides a highly accurate treatment of the advection terms.[1] Scheme 3 uses mixed interpolation on a staggered Arakawa C-grid. Since it uses piecewise constant basis functions for some of the fields, the accuracy is less than that of scheme 1. Schemes 3P and 3T are hybrid schemes which use scheme 1 for the advection terms and scheme 3 for the gravity wave terms. Petrov–Galerkin treatment for the gravity wave terms is used with 3P, and 3T is based on the back-transformation method. The time discretization is carried out by using the leap-frog scheme:

$$\psi^{n+1}_v = \psi^{n-1}_v + \psi^n_{tv} \cdot 2\Delta t, \tag{21}$$

with n denoting the time level. Since one-dimensional solutions are numerically much more stable than two- or three-dimensional solutions, we do not employ a space or time filter, which for higher-dimensional models is necessary to maintain stability.

Simulation of the Rossby wave

The first test is the simulation of the Rossby wave (3). We use a regular grid with $\Delta t = 200$ s, grid length $\Delta X = 400\,000$ m, 19 independent grid points, periodic boundary conditions and $F_0 = 0$. The initial velocity fields are chosen to satisfy the geostrophic balance condition

$$\begin{aligned} V &= H_X/f, \\ U &= -H^0_Y/f, \end{aligned} \tag{22}$$

with $H^0_Y = 0{\cdot}01\ \mathrm{m\,s^{-2}}$ and, $f = 0{\cdot}0001\ \mathrm{s^{-1}}$. The forecast time was chosen such that just one rotation is performed. Figure 2 shows the initial H-field and forecasts using schemes 1, 2, 3 and 3P. Scheme 1 has a much better accuracy than the second-order finite different scheme 2. Also the accuracy of scheme 3 is not good enough, being about the same as that of scheme 2. Scheme 3P, however, which uses the lower-order treatment only for the gravity wave terms, gives a similar quality of Rossby wave prediction as scheme 1.

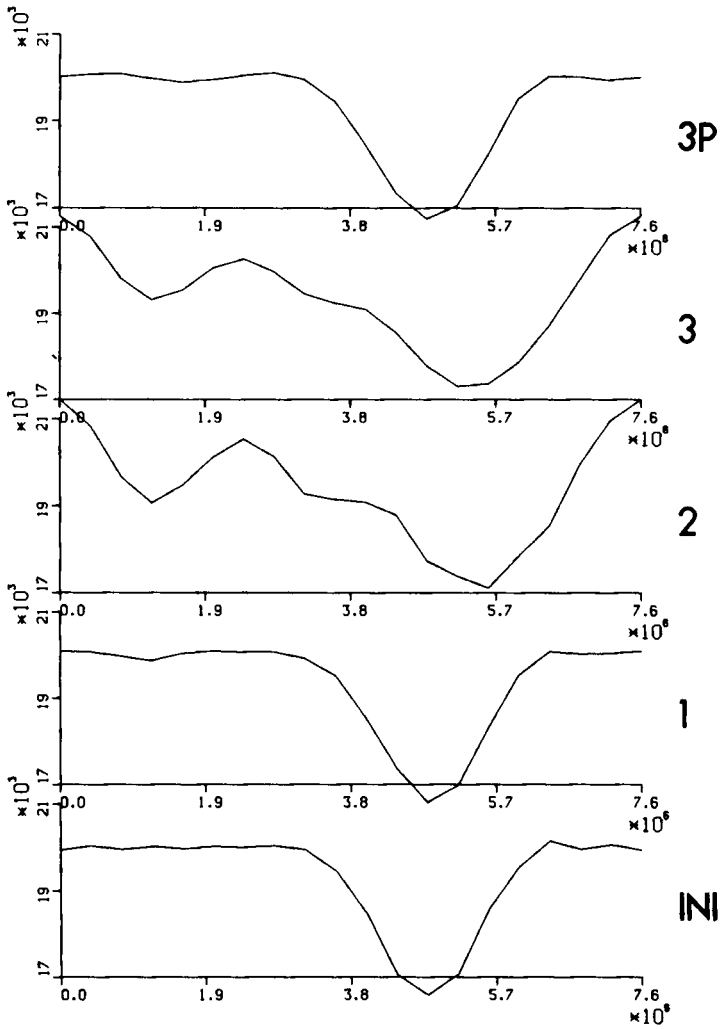

Figure 2. The initial H-field (INI) and forecasts using schemes 1, 2, 3 and 3P

Geostrophic adjustment and irregular resolution

The advantages of the staggered scheme 3 were established with respect to the geostrophic adjustment process.[7,8] An example of adjustment is obtained by using (2) with a non-zero mountain forcing function F_0. We also want to test the performance on irregular grids.

In combination with an error estimator model, a variable resolution can be used to refine the resolution selectively in regions where an increased accuracy is needed. In an important paper, Skamarock *et al.*[21] have shown that adaptive mesh refinement is possible using standard numerical schemes. Numerical problems at the boundary between the coarse and fine meshes can be avoided if the boundary is in regions of a low error estimate for the coarse mesh, which corresponds physically to regions of smooth fields. However, for operational use it may be necessary to ask for robust schemes, which also work properly when the boundaries do not all conform to this requirement.

The question of robustness of a scheme is even more important when considering nested models like that described in Reference 14 with a fixed region of high resolution. This region is determined by the interest of the user of the model rather than by an error estimate. For such models it is clearly necessary that there are no numerical noise problems caused by the boundary between coarse and fine mesh. In particular, the forcing fields, such as orography, are in current models defined on the smallest scales in order to obtain as much local detail of the forecast as possible. The test calculations described in the following are designed to investigate the robustness of numerical schemes in the presence of small-scale forcing.

For our experiments we use 23 independent grid points, with

$$\Delta X_{\nu+1/2} = \begin{cases} X_{\nu+1} - X_\nu = 200\,000 \text{ m} & \text{for } \nu \in \{3, \ldots, 10\}, \\ 400\,000 \text{ m} & \text{elsewhere.} \end{cases} \tag{23}$$

The initial values are

$$\begin{aligned} H &= H_0 = 20\,000 \text{ m}^2 \text{ s}^{-2}, \\ U &= U_0 = -H_Y^0/f, \\ V &= 0, \end{aligned} \tag{24}$$

with $H_Y^0 = 0{\cdot}01 \text{ m s}^{-2}$ and $f = 0{\cdot}0001 \text{ s}^{-1}$.

A first set of experiments was done using a single small-scale mountain in a uniformly resolving part of the grid, defined by

$$\begin{aligned} F_{0_{12}} &= 7000 \text{ m}^2 \text{ s}^{-2}, \\ F_0 &= 0 \quad \text{elsewhere.} \end{aligned} \tag{25}$$

The formulae above refer to equation (10).

There exists a stationary solution for this problem[22] which can be given in parametric form, with w being an arbitrary function:

$$\begin{aligned} U(X) &= U_0/(1 - w_{XX}), \\ V(X) &= -fw_X, \\ H(X) &= -U^2/2 - f^2 w + (U_0^2/2 + H_0), \\ F_0(X) &= H - H_0 U_0/U. \end{aligned} \tag{26}$$

The stationary state is approximated by performing 4000 time steps with $\Delta t = 200$ s and averaging this in time. After this procedure we perform another 4000 time steps, and the solution is shown in Figures 3–5 for schemes 1, 2 and 3P respectively.

The forecast with scheme 1 (Figure 3) shows that the solution is contaminated with some small-scale features, the so-called noise. Even though a very extended time interval was used to prepare the initial state by averaging, the solution is not stationary with respect to the noise features. The same is true for the computation with scheme 2 (Figure 4). However, this less accurate scheme has much more noise. The best results are obtained by scheme 3P (Figure 5). The amplitude of the non-stationary noise has become very small. The results described in Figures 3–5 are consistent with theoretical results[10] as applied to the schemes investigated in Reference 8.

One motivation for grid refinement is the introduction of a physical forcing in the small scale. A further set of experiments was carried out by replacing the mountain forcing given by (25) by a

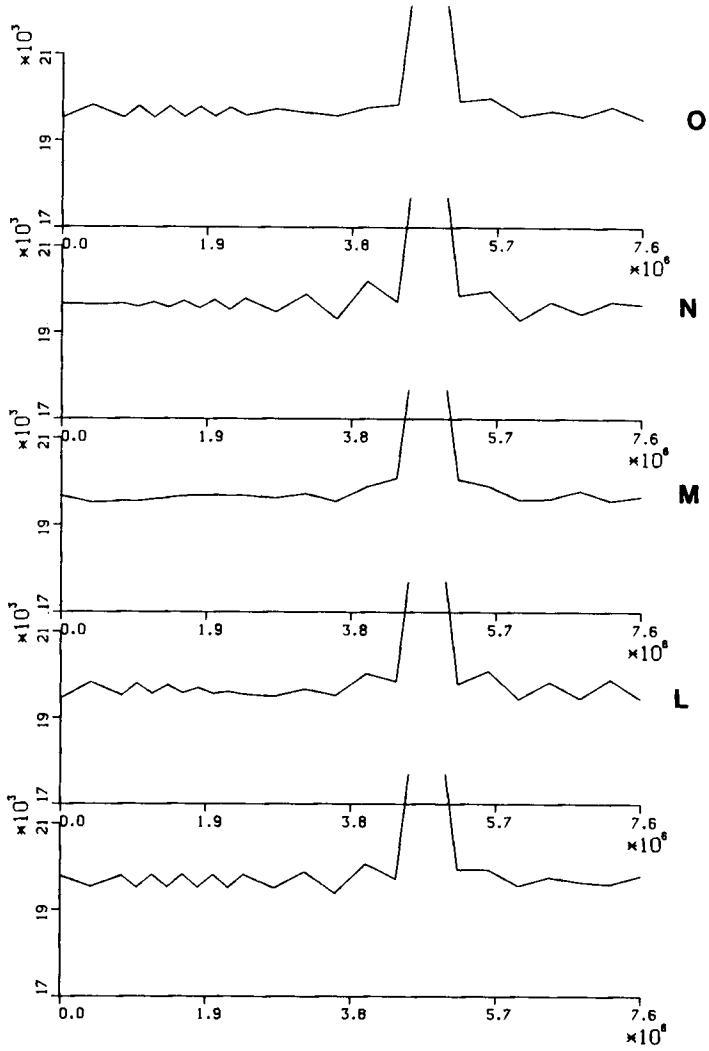

Figure 3. Computation of the stationary flow in the presence of a mountain forcing by scheme 1. The initial state (bottom) was prepared by time-averaging a forecast of 4000 steps. The forecasted H-fields are shown after 1000 (L), 2000 (M), 3000 (N) and 4000 (O) steps

mountain which is situated near the boundary of the coarse and the fine mesh:

$$F_{o10} = 7000\ \mathrm{m^2\,s^{-2}},$$

$$F_o = 0 \quad \text{elsewhere.} \tag{27}$$

Since we are now dealing with a situation of irregular resolution, no theoretical results concerning the behaviour of discretizations are available, except those describing the simulation of stationary states.[5] These results favour the use of staggered schemes such as our scheme 3. The initial state is again prepared by time-averaging a forecast of 4000 steps.

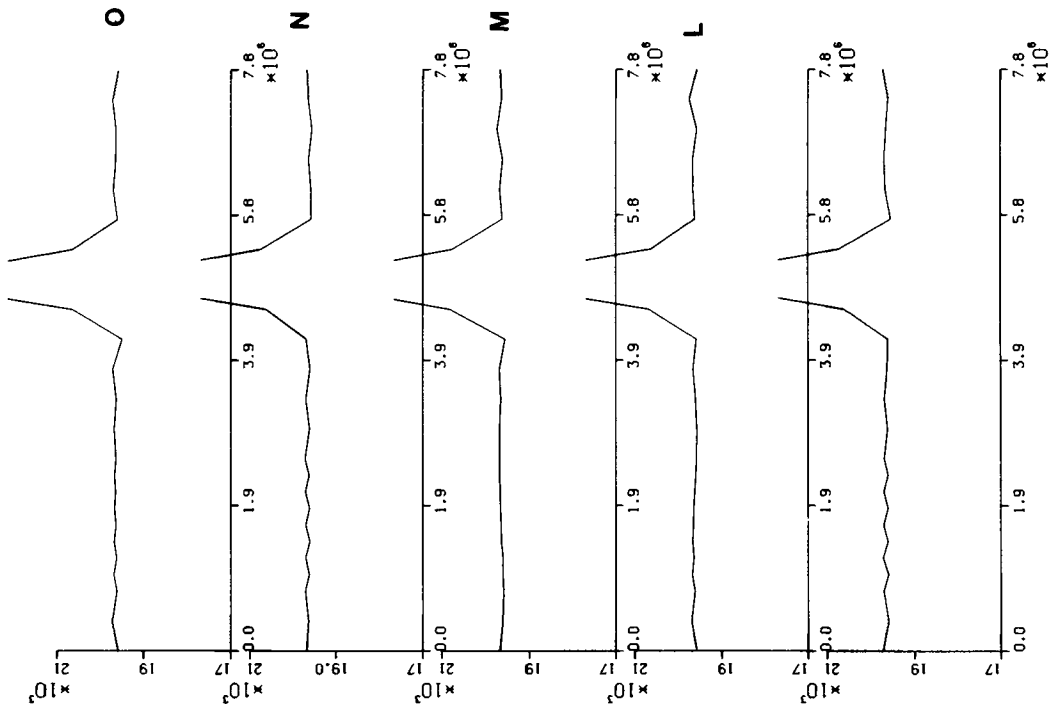

Figure 5. As Figure 3, for scheme 3P

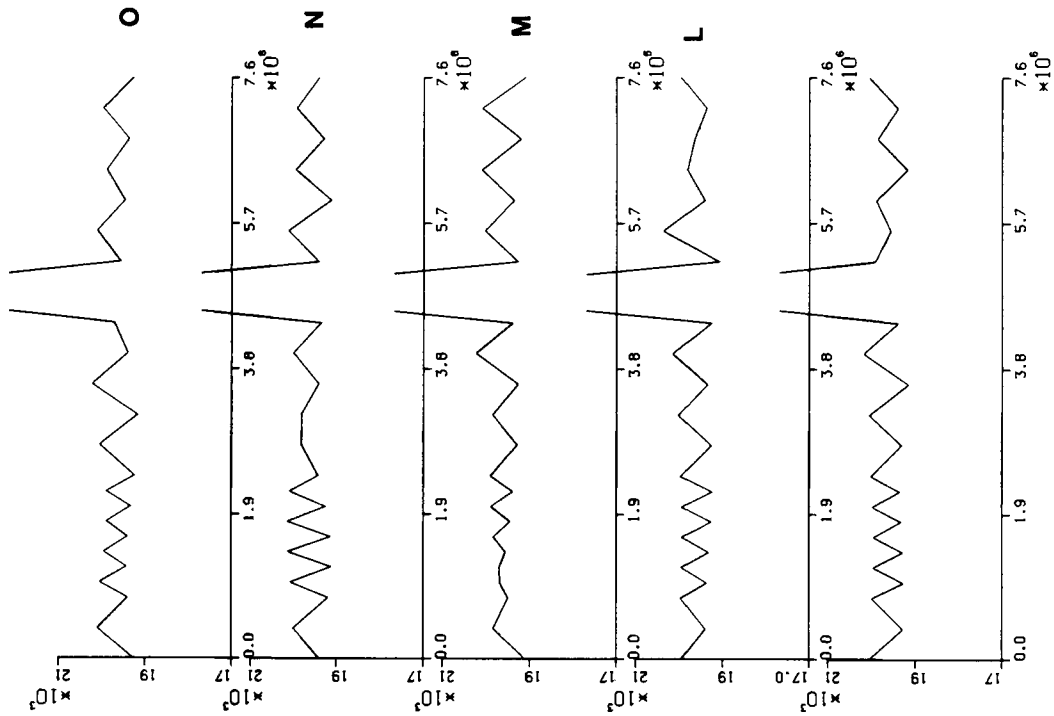

Figure 4. As Figure 3, for scheme 2

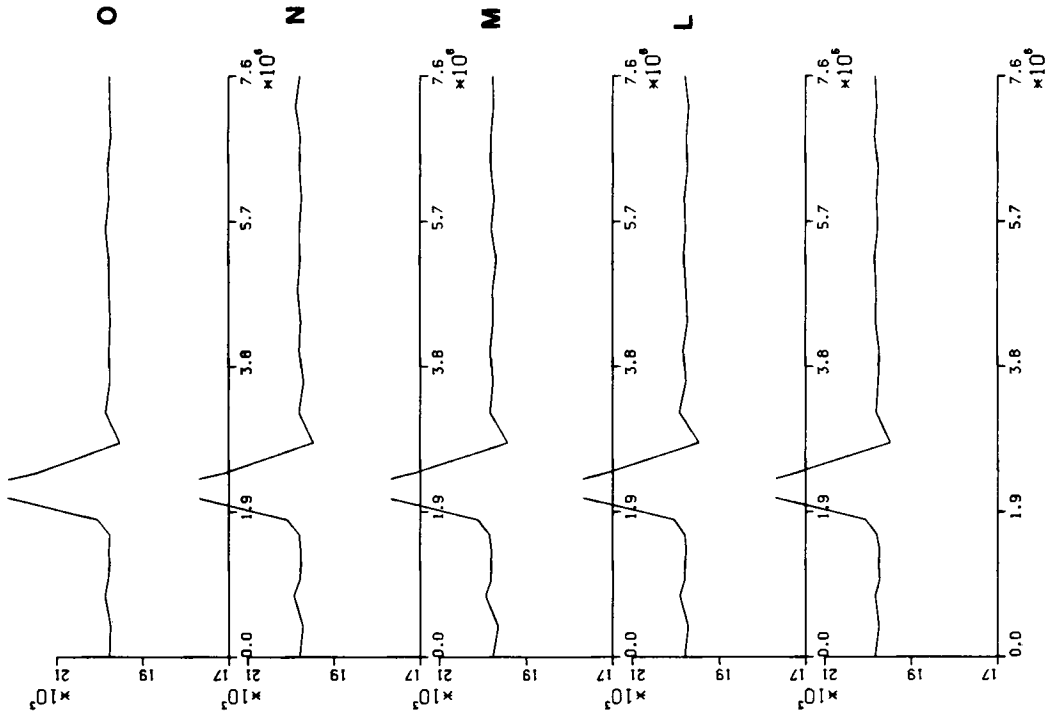

Figure 6. As Figure 3, with the mountain near the boundary of the coarse and the fine mesh,

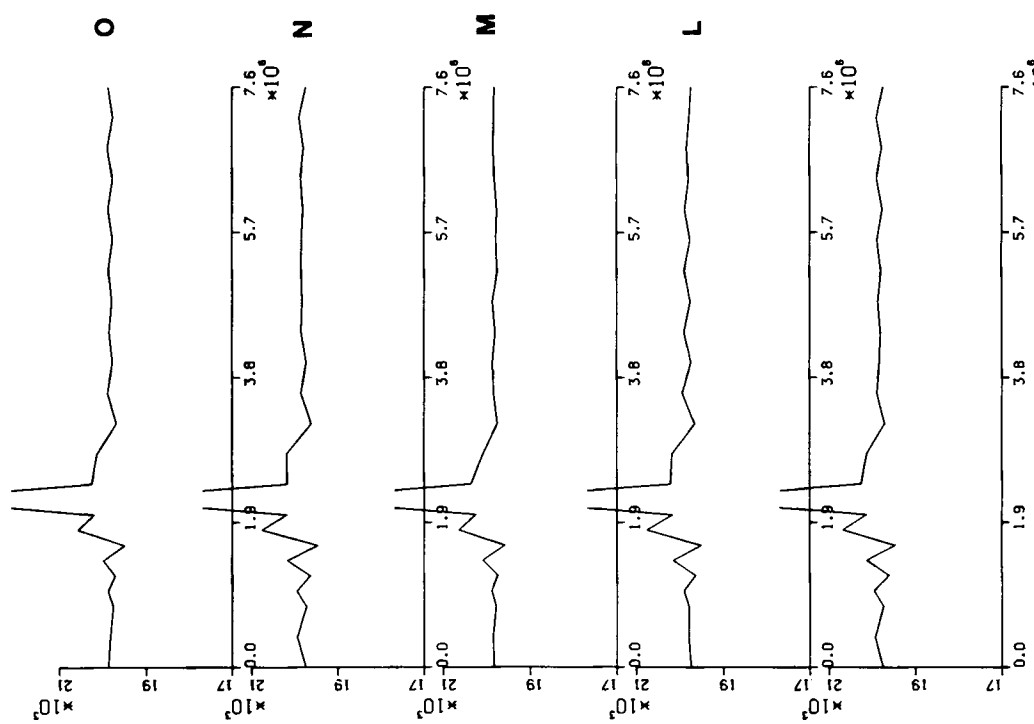

Figure 7. As Figure 6, for scheme 3

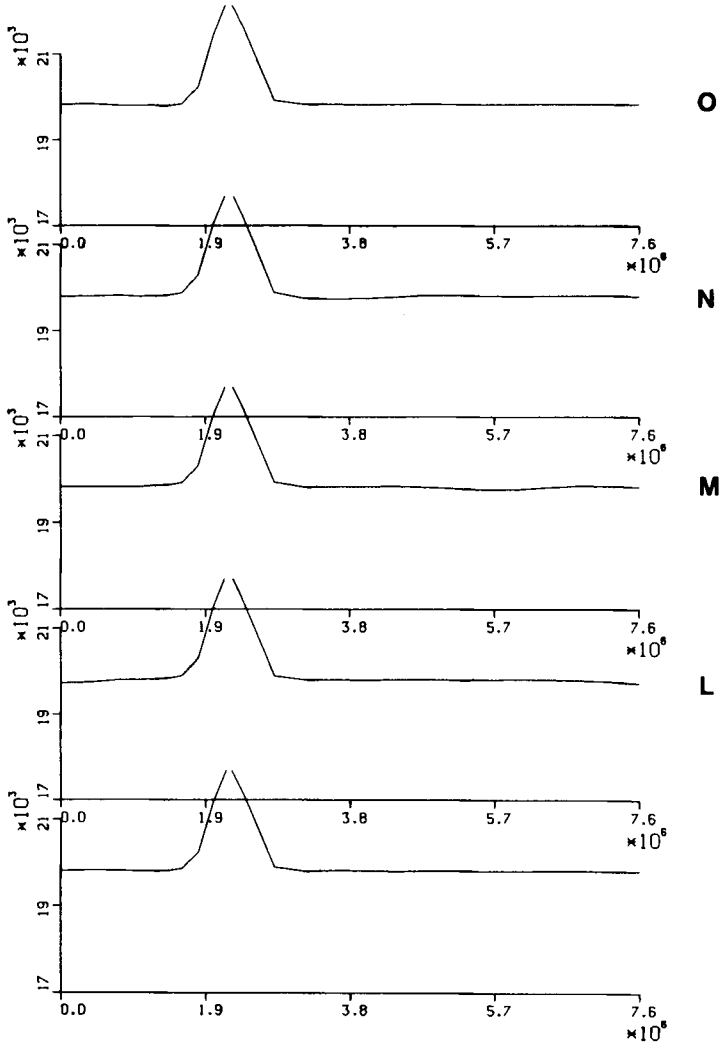

Figure 8. As Figure 6, for scheme 3T

The forecast for scheme 1 is shown in Figure 6. As in Figure 3 there is some noise, which this time is limited to the fine mesh region. There is no indication that the presence of irregular resolution in the region of forcing leads to a deterioration of the results as compared to Figure 3.

Scheme 3P is unsuitable for this situation since it leads to considerable noise. The results of scheme 3 (Figure 7) are quite good. However, as we have seen in Figure 2, this scheme does not have a suitable accuracy for the computation of the transient Rossby wave.

The hybrid scheme 3T, based on the incorporation of scheme 3 by back-interpolation, works well for this problem. The result (Figure 8) shows a rather good representation of the geostrophic adjustment process.

In order to demonstrate that scheme 3T is also suitable for the treatment of the transient features of atmospheric flow, Figure 9 shows the prediction of a Rossby wave. The physical

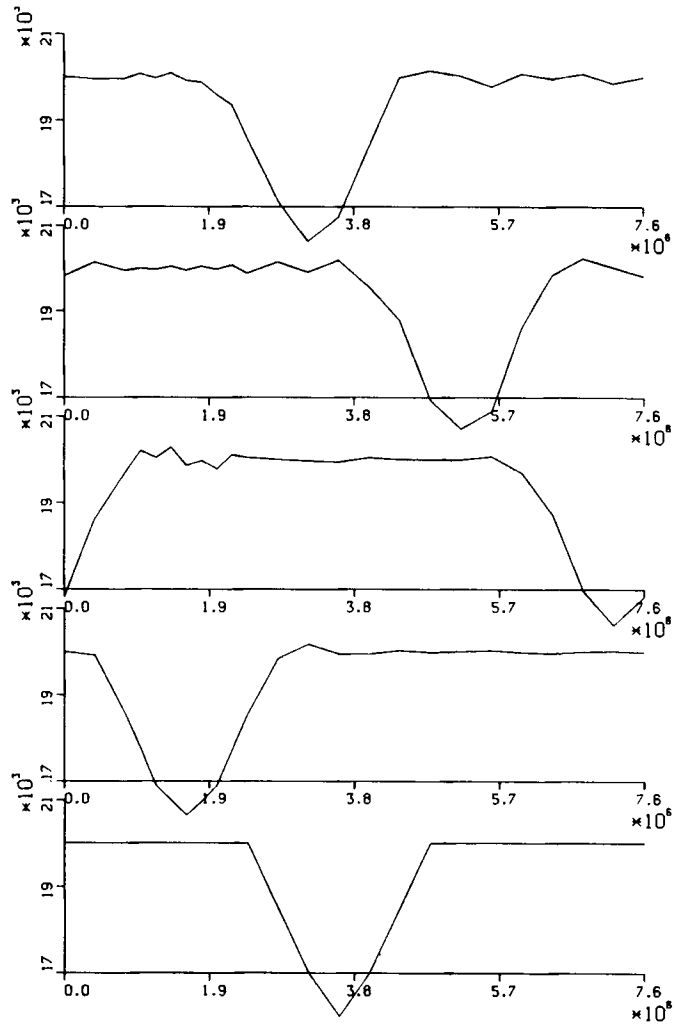

Figure 9. Forecast of a Rossby wave in an irregular grid by scheme 3T with $\Delta t = 200$ s. The initial and forecasted H-fields are shown after 100 (I), 200 (M), 300 (N) and 400 (O) time steps

situation is as in Figure 3, but the grid length is halved between grid points 3 and 11, as described in (23). The accuracy of simulation is comparable to that of the accurate scheme 1 (and 3P) in Figure 3. The irregularity of the grid does not seem to cause special problems. The inaccuracy of simulation seen in Figure 9 is consistent with that encountered in the advection process.[1] However, since our system contains fast-moving gravity waves, the errors have spread over the whole domain rather than being concentrated near the trough.

5. CONCLUSIONS

Numerical schemes for atmospheric simulation are required to simulate transient features accurately as well as to give a noise-free representation of quasi-stationary states. The first

requirement demands a high enough order of approximation, while the second makes it necessary that the scheme has a physically reasonable behaviour also near the limit of resolution.

The hybrid finite element schemes 3P and 3T match these two requirements by combining an unstaggered treatment of the advection terms with an approximation of the gravity wave terms in the Arakawa C-grid. Test computations of a transient Rossby wave and a geostrophic adjustment process have been provided to demonstrate this effect. The hybrid scheme 3T also shows good behaviour for an irregular grid.

APPENDIX I: TRANSFER FUNCTION ANALYSIS

The transfer function analysis, as developed in References 9, 10 and 19, is a theory which can analyse the main source of the noisiness of numerical schemes. It has been applied to the analysis of numerical schemes[7,8,20,23] and is based on earlier work presented in Reference 24. The method applies to linear space-invariant systems. An output signal $Y_o(X)$ of a system is related to an input signal $Y_i(X)$. Denote the Fourier transforms as $\tilde{Y}_i(k)$ and $\tilde{Y}_o(k)$:

$$\tilde{Y}_i(k) = \int Y_i(X)e^{-ikX}dX,$$

$$\tilde{Y}_o(k) = \int Y_o(X)e^{-ikX}dX. \tag{28}$$

Input and output are related by

$$\tilde{Y}_o(k) = \tilde{\phi}(k)\,\tilde{Y}_i(k). \tag{29}$$

When $\tilde{\phi}(k)$ is known, the signal deformation can be analysed. In numerical systems the impact of the numerical discretization error on signal propagation can be investigated.

Writing $\tilde{\phi}$ as

$$\tilde{\phi}(k) = |\tilde{\phi}(k)|e^{i\alpha_k}, \tag{30}$$

the propagation error can be analysed as amplitude error arising from $|\tilde{\phi}(k)|$, and phase error which comes from $\exp(i\alpha_k)$. For meteorological application we consider the linearized gravity wave equations as a linear filter. The basis equations are obtained by linearizing (1) in an infinite domain with no mean flow:

$$\begin{aligned} \partial u/\partial t - fv + \partial h/\partial X &= 0, \\ \partial v/\partial t + fu &= 0, \\ \partial h/\partial t + H\,\partial u/\partial X &= 0, \end{aligned} \tag{31}$$

where u, v and h are pertubation velocities and heights, and H is the mean height.

Introducing Fourier transforms

$$U(k,t) = \int U(X,t)e^{-ikX}dX, \tag{32}$$

etc., we obtain from (31)

$$\begin{aligned} \partial\tilde{u}/\partial t &= f\tilde{v} - ik\tilde{h}, \\ \partial\tilde{v}/\partial t &= -f\tilde{u}, \\ \partial\tilde{h}/\partial t &= -ikH\tilde{u}, \end{aligned} \tag{33}$$

with initial condition

$$\tilde{u}_i = \tilde{u}(k, 0) = \int U(X, 0) e^{-ikX} dX, \tag{34}$$

etc. The solution of (33) is given in Reference 9 and was analysed with respect to amplitude and wave propagation errors. Amplitude deformation of a numerical scheme is more difficult to analyse. It has to be required that the overall solution is damped for wave numbers for which it is inaccurate. A specially designed explicit diffusion will be necessary in most cases. We consider here only wave velocity errors. For solutions of the form

$$\begin{pmatrix} u \\ v \\ h \end{pmatrix} = \mathrm{Re}\left(\begin{pmatrix} u_0 \\ v_0 \\ h_0 \end{pmatrix} + \begin{pmatrix} u_1 \\ v_1 \\ h_1 \end{pmatrix} e^{i\nu t} \right), \tag{35}$$

we obtain[9] for the frequencies

$$\nu = (f^2 + k^2 H)^{1/2}.$$

For the finite element approximations defined in (7) and (8) the approximation of (33) takes the form

$$\begin{aligned} \alpha d\tilde{u}/dt &= \alpha f v - i\mu g \tilde{h}, \\ \alpha d\tilde{v}/dt &= -\alpha f \tilde{u}, \\ \gamma d\tilde{h}/dt &= -i\mu H \tilde{u}. \end{aligned} \tag{36}$$

For the approximated frequencies ν_2 we obtain

$$\nu_a = (f^2 + \mu^2 H/\alpha\gamma)^{1/2}.$$

We consider the phase and group velocities C_p and C_g of our system:

$$\begin{aligned} C_p &= \nu/k, \\ C_g &= \partial\nu/\partial k. \end{aligned} \tag{37}$$

For the approximated system we obtain

$$\begin{aligned} C_p^a &= \nu_a/h, \\ C_g^a &= \partial\nu_a/\partial k. \end{aligned} \tag{38}$$

The balanced state of the atmosphere is assumed by the process of geostrophic adjustment. This can only be properly represented if the numerical approximation does not reverse the sign of the group velocity.[9,10]

We have therefore as a necessary condition a numerical scheme

$$C_g^a C_g \geqslant 0. \tag{39}$$

For schemes 1, 2 and 3 the evaluation of (37) was carried out in Reference 8, and scheme 3 proved to be a suitable discretization. Since we are interested in grid lengths $\Delta X = 100$ km or smaller, it is reasonable to consider the case $f = 0$.

For the Petrov–Galerkin schemes 2P and 3P the evaluation of (37) is given in Table II, showing that both schemes are suitable with the Petrov–Galerkin approach, even though 2P is an unstaggered scheme. For scheme 2P an increase of wave velocities above the analytic values is

Table II. Relative group velocities C_g^a/C_g as function of wave number

$k\Delta X/\pi$	Scheme 2P C_g^a/C_g	Scheme 3P C_g^a/C_g
0·4	1·53	1·2
0·6	2·9	1·39
0·8	10·5	1·23
1·0	—	0

noted, which is singular for $k\Delta X/\pi \to 1$. With explicit time integration schemes, CFL problems may be expected, but using the semi-implicit method, scheme 2P is suitable and has been used in Reference 11.

APPENDIX II: LIST OF SYMBOLS

$C_\rho(X)$	basis function
$\bar{C}_\rho(X)$	basis function for Petrov–Galerkin method
$e_\rho(X)$	linear spline basis function in one space dimension
f	Coriolis parameter
$M_{v,i}$	mass matrix
RS	right-hand side of dynamic equations
t	time
U, V	velocity components in X- and Y-direction
X	space co-ordinate
$\underset{\sim}{\psi}(X)$	field
$\tilde{\psi}(X)$	field in approximation space
$\chi_v(X)$	piecewise constant basis function in one space dimension
ΔX	grid length

REFERENCES

1. P, M. Gresho, R. L. Lee and R. L. Sani, 'Advection-dominated flows, with emphasis on the consequences of mass lumping', *Finite Elements in Fluids, Vol. 3*, Wiley, New York, 1977, pp. 335–350.
2. A. N. Staniforth, 'The application of the finite-element method to meteorological simulations—A review', *Int. j. numer. methods fluids*, **4**, 1–22 (1984).
3. I. M. Navon, 'FEUDX, a two-stage high accuracy finite element Fortran program for solving the shallow water equations', *Comput. Geosci.*, **13**, 255–285 (1987).
4. D. J. Carson and M. J. P. Cullen, 'Intercomparison of short-range numerical forecasts using finite difference and finite element models from U.K. Meteorological Office', *Beitr. Phys. Atmos.*, **50**, 1–15 (1977).
5. R. L. Sani, P. M. Gresho, R. L. Lee and D. F. Griffiths, 'The cause and cure (?) of the spurious pressures generated by certain FEM solutions of the incompressible Navier–Stokes equations, Part 1', *Int. j. numer. methods fluids*, **1**, 17–43 (1981).
6. R. L. Sani, P. M. Gresho, R. L. Lee, D. F. Griffiths and M. Engelman, 'The cause and cure (!) of the spurious pressures generated by certain FEM solutions of the incompressible Navier–Stokes equations, Part 2', *Int. j. numer. methods fluids*, **1**, 171–204 (1981).
7. R. T. Williams and O. C. Zienkiewicz, 'Improved finite element forms for the shallow water wave equations', *Int. j. numer. methods fluids*, **1**, 81–97 (1981).
8. J. Steppeler, 'Analysis of group velocities of various finite element schemes', *Beitr. Phys. Atmos.*, **62**, 151–161 (1989).
9. A. Schoenstadt, 'A transfer function analysis of numerical schemes used to simulate geostrophic adjustment', *Mon. Weather Rev.*, **108**, 1248–1259 (1980).

10. R. T. Williams, 'On the formulation of finite element prediction models', *Mon. Weather Rev.*, **109**, 463–466 (1981).
11. J. Côte and A. N. Staniforth, 'Eliminating the Poisson problems in semi-implicit unstaggered primitive equation models', *Research Activities in Atmospheric Oceanic Modelling II*, *WMO/TD No. 263*, 1989.
12. A. Arakawa, 'Computational design for long term numerical integration of the equation of fluid motion: 1. Two-dimensional incompressible flow', *J. Comput. Phys.*, **1**, 119–143 (1966).
13. A. N. Staniforth and H. L. Mitchell, 'A semi-implicit finite element barotropic model', *Mon. Weather Rev.*, **105**, 154–169 (1977).
14. N. A. Phillips, 'The nested grid model', *NOAA Tech. Rep. NWS 22*, 1979, p. 79.
15. J. Steppeler, 'A Galerkin finite element–spectral weather forecast model in hybrid coordinates', *Comput. Math. Appl.*, **16**, 23–30 (1988).
16. J. Steppeler, 'Quadratic Galerkin finite element schemes for the vertical discretization of numerical forecast models', *Mon. Weather Rev.*, **115**, 1575–1588 (1988).
17. J. Steppeler, 'A cubic spline Galerkin scheme for the vertical discretization of atmospheric models', *Q. J. R. Soc.*, **114**, 1545–1561 (1988).
18. B. Neta and R. T. Williams, 'Stability and phase-speeds for various finite element formulations of the advection equation', *Comput. Fluids*, **14**, 393–410 (1989).
19. A. Schoenstadt, 'The effect of spatial discretization on the steady state and transient behaviour of the dispersive wave equation', *J. Comput. Phys.*, **23**, 364–379 (1977).
20. B. Neta and I. M. Navon, 'Analysis of the Turkel–Zwas scheme for the shallow water equations', *J. Comput. Phys.*, **81**, 277 (1989).
21. W. Skamarock, J. Oliger and R. L. Street, 'Adaptive grid refinement for numerical weather prediction', *J. Comput. Phys.*, **80**, 27 (1989).
22. W. Edelmann, 'An analytic solution for stationary barotropic flow crossing a meridional mountain barrier', *Beitr. Phys. Atmos.*, **45**, 87–93 (1972).
23. R. C. Wajsowicz, 'Free planetary waves in finite-difference numerical models', *J. Phys. Oceanogr.*, **16**, 773–789 (1986).
24. R. Grotjahn and J. J. O'Brien, 'Some inaccuracies in finite differencing hyperbolic equations', *Mon. Weather Rev.*, **104**, 180–194 (1974).
25. A. N. Staniforth and R. W. Daley, 'A finite-element formulation for the vertical discretization of sigma coordinate primitive equation model', *Mon. Weather Rev.*, **105**, 1108–1118 (1977).